Supplemental Information

DOCK6 promotes chemo- and radio-resistance of gastric cancer by modulating WNT/β-catenin signaling and cancer stem cell traits

Hsiang-Cheng Chi[1, 2, 3]*, Chung-Ying Tsai[4]*, Chia-Siu Wang[5]*, Huang-Yu Yang[6, 7, 8]*, Chien-Hui Lo[9,10], Won-Jing Wang[9,10], Kam-Fai Lee[11], Li-Yin Lai[12], Ji-Hong Hong[13], Yen-Fang Chang7, Ming-Ming Tsai[5, 14, 15], Chau-Ting Yeh[16], Cheng Heng Wu[2], Ching-Chuan Hsieh[5], Lu-Hai Wang[3, 17]*, Wei-Jan Chen[18]* and Kwang-Huei Lin[2, 15, 16]*

Supplemental materials

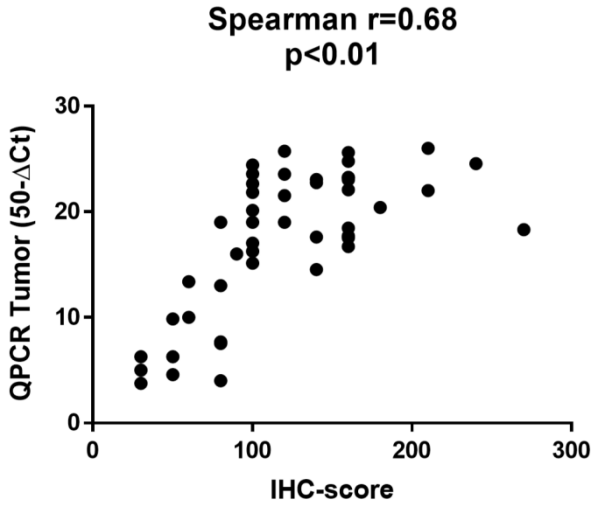

Supplemental Figure 1. Expressions of *DOCK6* mRNA and DOCK6 protein in clinical GC specimens displayed a positive correlation.

47 samples contain both RNA and Formalin-fixed paraffin-embedded from the same gastric tumors were used to determine the association between DOCK6 mRNA and protein expressions.

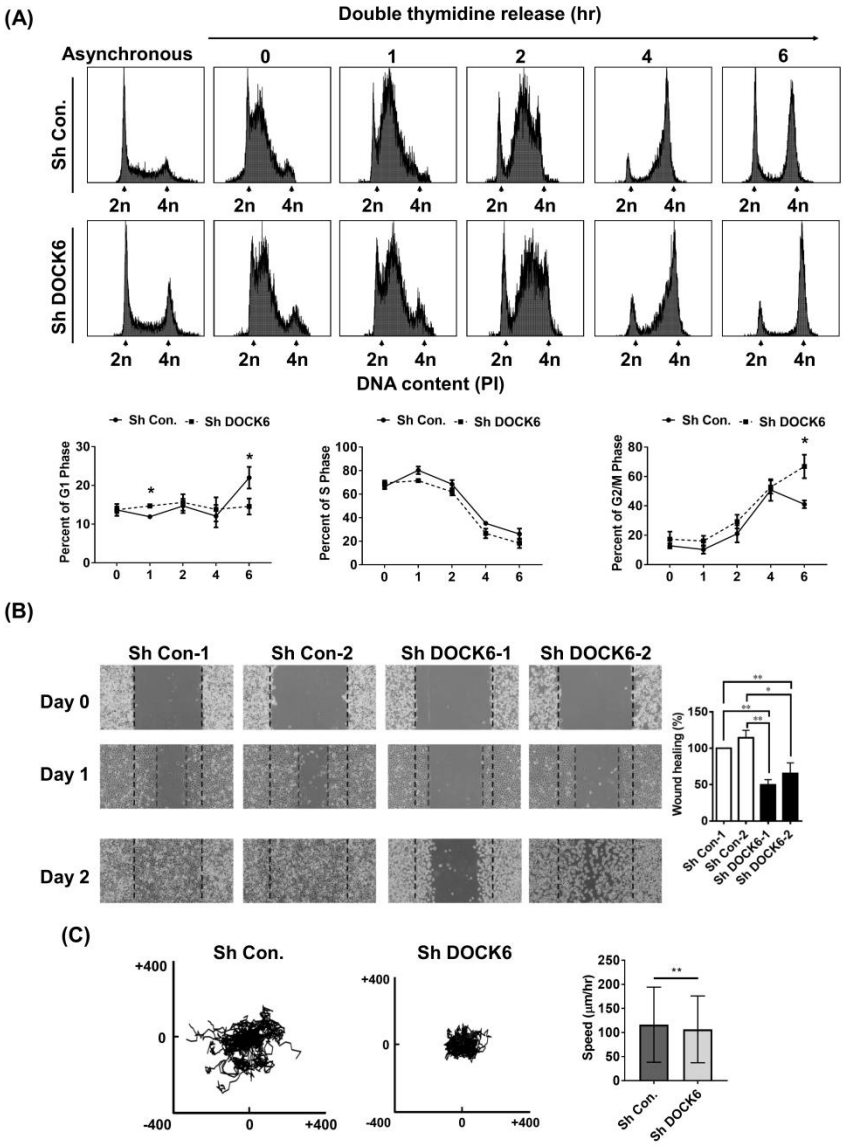

Supplemental Figure 2. Depletion of DOCK6 decreased cell cycle progression and migration of GC cells

(A) Cell cycle progression of the synchronized DOCK6-silenced and control cells. The cells were synchronized in G1/S transition by thymidine double block. Synchronized cells were cultured in fresh RPMI containing 10% FBS, collected at indicated time after released from G1/S boundary, analyzed by flow cytometry. The percentage of cell cycle distribution at the indicated time is presented in the lower panel. (n=3), * $p<0.05$. (B) Quantification of the wound healing assay. The left panel represents phase-contrast images of the wound healing assay at 0, 1 and 2 days after scratching. (C) Tracking a single cell migration in control and DOCK6-silenced GC cells. Wind-rose plots shown the migration paths of 60 individual control and DOCK6-silenced cells captured in a time-lapse motility assay (The data was pooled from three independent experiments). The right panel showed the migration speed (total length of the migration path per hour) of these tracked cells. * $p<0.01$

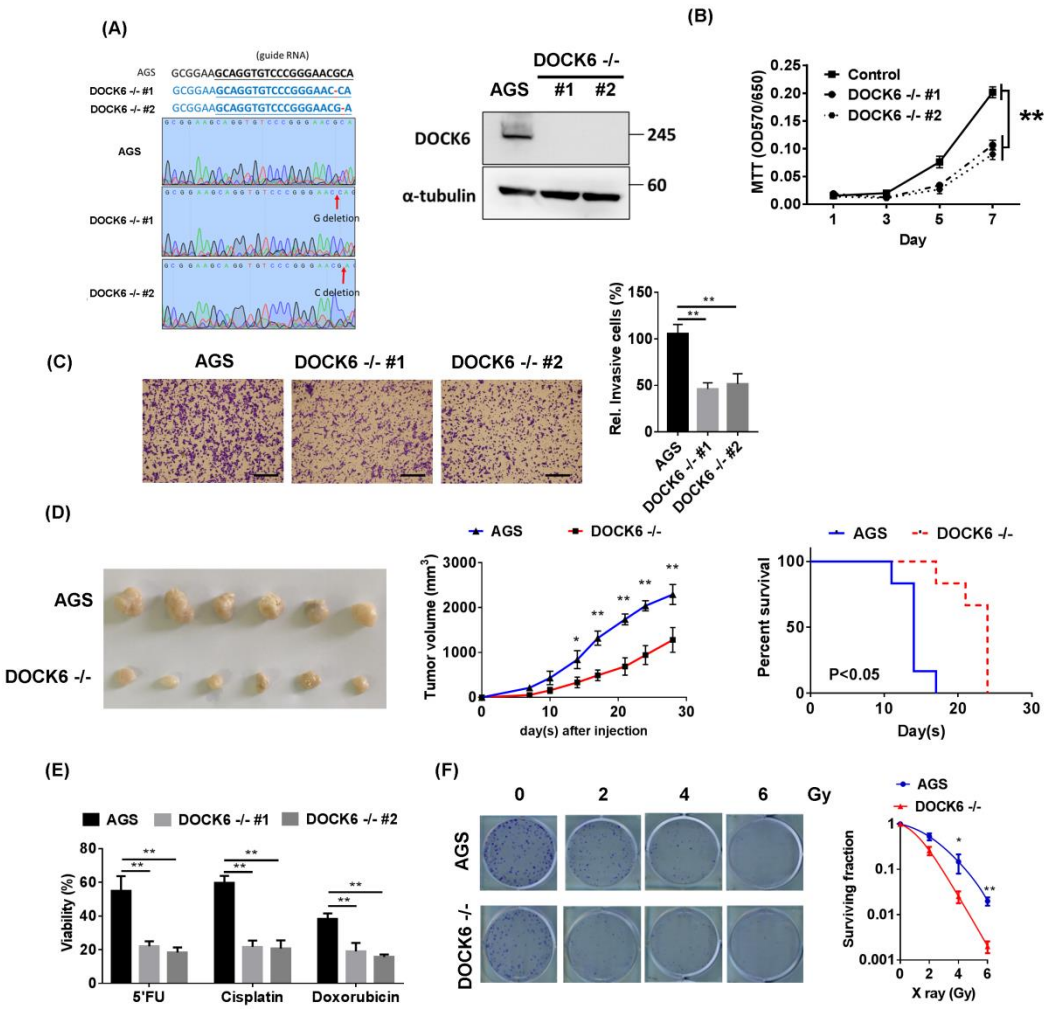

Supplemental Figure 3. DOCK6 depletion suppresses proliferation and metastasis of GC cells.

(A) The efficiency of DOCK6 silencing in AGS cells determined via immmuno-blotting. Genotyping performed to reveal the edited alleles in *DOCK6* gene was shown as the left panel. (B) Measurement of cell growth curves with the MTT assay. (C) Transwell invasion assay of control and DOCK6-/- AGS cells. Right panel: quantified result. (Scale bar, 200 μm) (D) DOCK6-knockout and control AGS cells ($2x10^6$) were subcutaneously injected into nude mice for observation of tumor growth. After sacrifice, tumors from these groups of mice (n=6 for each group) were collected. (* $p<0.05$, **$p<0.01$). Kaplan-Meier plots using standard tumor sizes ($600mm^3$) as a criterium for euthanasia. (E) Chemoresistance was determined based on the relative number of surviving cells after treatment with 5'FU (20 μg/ml)), cisplatin (3 μM) or doxorubicin (1 μM). Cell survival was examined using the MTT method. (F) Representative photographs showing the growth characteristics of cell colonies 10 days after X-ray irradiation. The right panel represents the calculated clonogenic cell survival fraction.

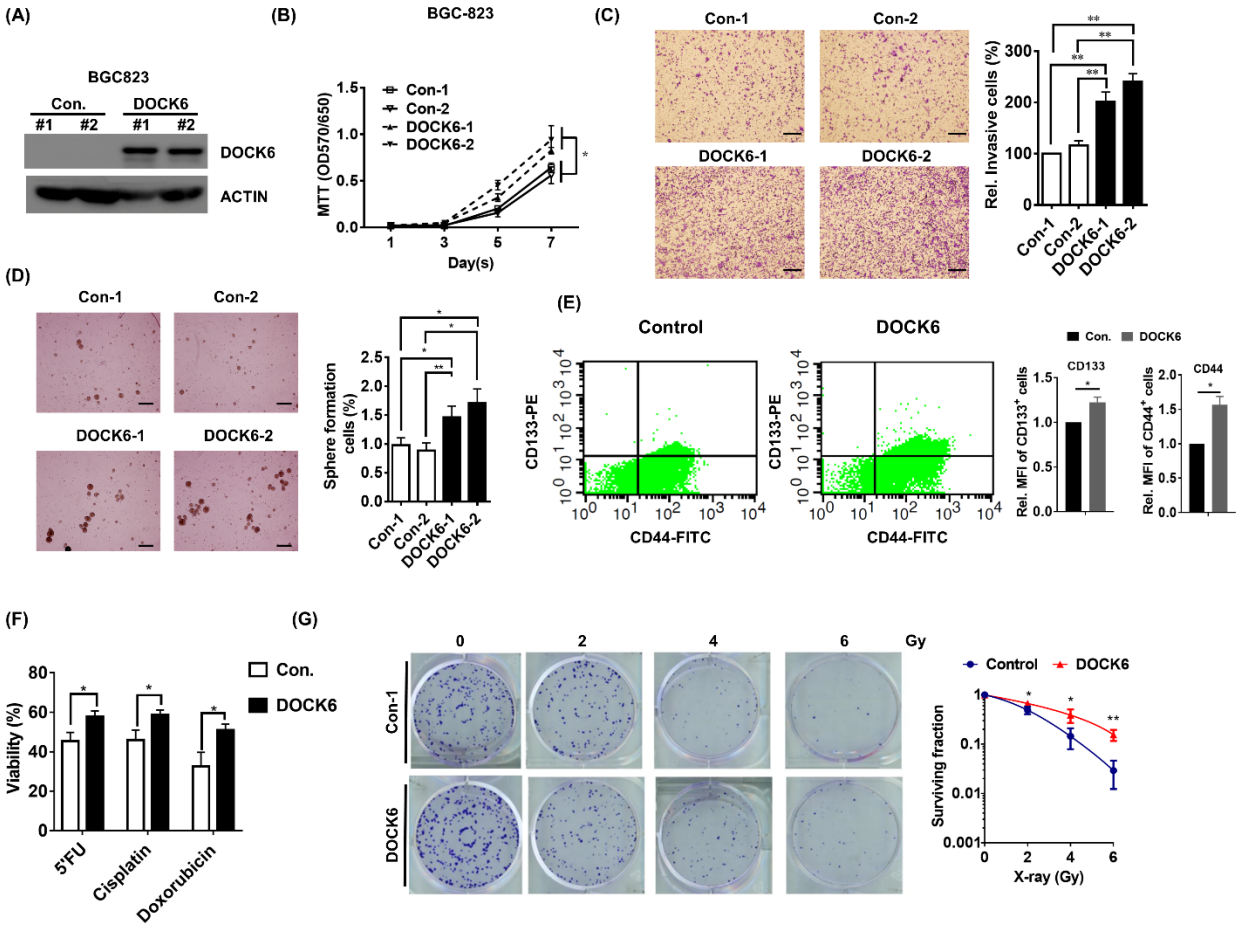

Supplemental Figure 4. Overexpression of DOCK6 promotes GC progression, chemo- and radioresistance, and stemness of BGC823 cells

(A) The efficiency of DOCK6 overexpression in BGC-823 cells was determined via western blot. (B) Measurement of the cell growth curve with the MTT assay. (C) Transwell invasion assay of DOCK6-overexpressing and control BGC-823 cells. Right panel: quantified result. Scale bar, 200μm. (D) DOCK6 overexpression promotes the capacity of oncosphere formation. Scale bar, 200μm. The right panel represents statistical results. (E) The representative plots from flow cytometry. The relative means of fluorescent intensities (MFI) of CD44-FITC and CD133-PE in $CD133^+$ or $CD44^+$ cells were shown in the lower panel. (F) Chemosensitivities of DOCK6-overexpressing and control BGC-823 cells were determined based on the relative number of surviving cells after treatment with 5'FU (20μg/ml), cisplatin (3μM) or doxorubicin (1μM) for 72h. Cell survival was examined using the MTT method. (G) The representative photographs showing the growth characteristics of cell colonies 10 days after X-ray irradiation. The right panel represents the calculated clonogenic cell survival fraction. * $p<0.05$, ** $p<0.01$.

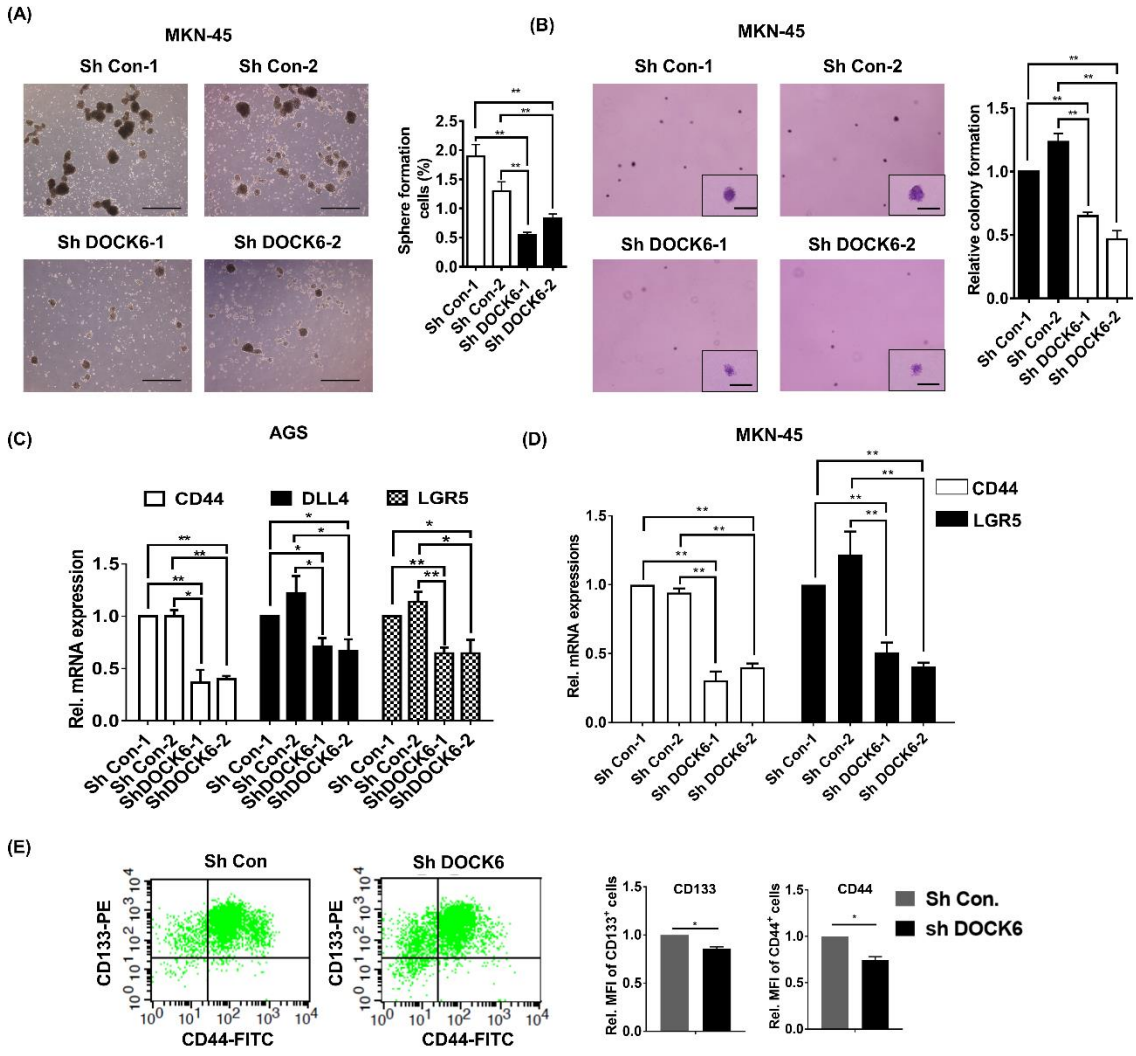

Supplemental Figure 5. Silence of DOCK6 suppresses stemness phenotypes of MKN-45 cells

(A) Knockdown of DOCK6 represses the capacity of oncosphere formation. Scale bar, 500μm. The right panel represents statistical results. (B) 3D colony formation ability of DOCK6-silenced and control MKN-45 cells. The right panel represents statistical results. Scale bar, 500μm (C, D) Q-RT-PCR analysis of the indicated molecules was determined in DOCK6-silenced and control AGS and MKN-45 cells, * $p<0.05$, ** $p<0.01$. (E) The representative plots from flow cytometry. The relative means of fluorescent intensities (MFI) of CD44-FITC and CD133-PE in $CD133^+$ or $CD44^+$ cells were shown in the lower panel.

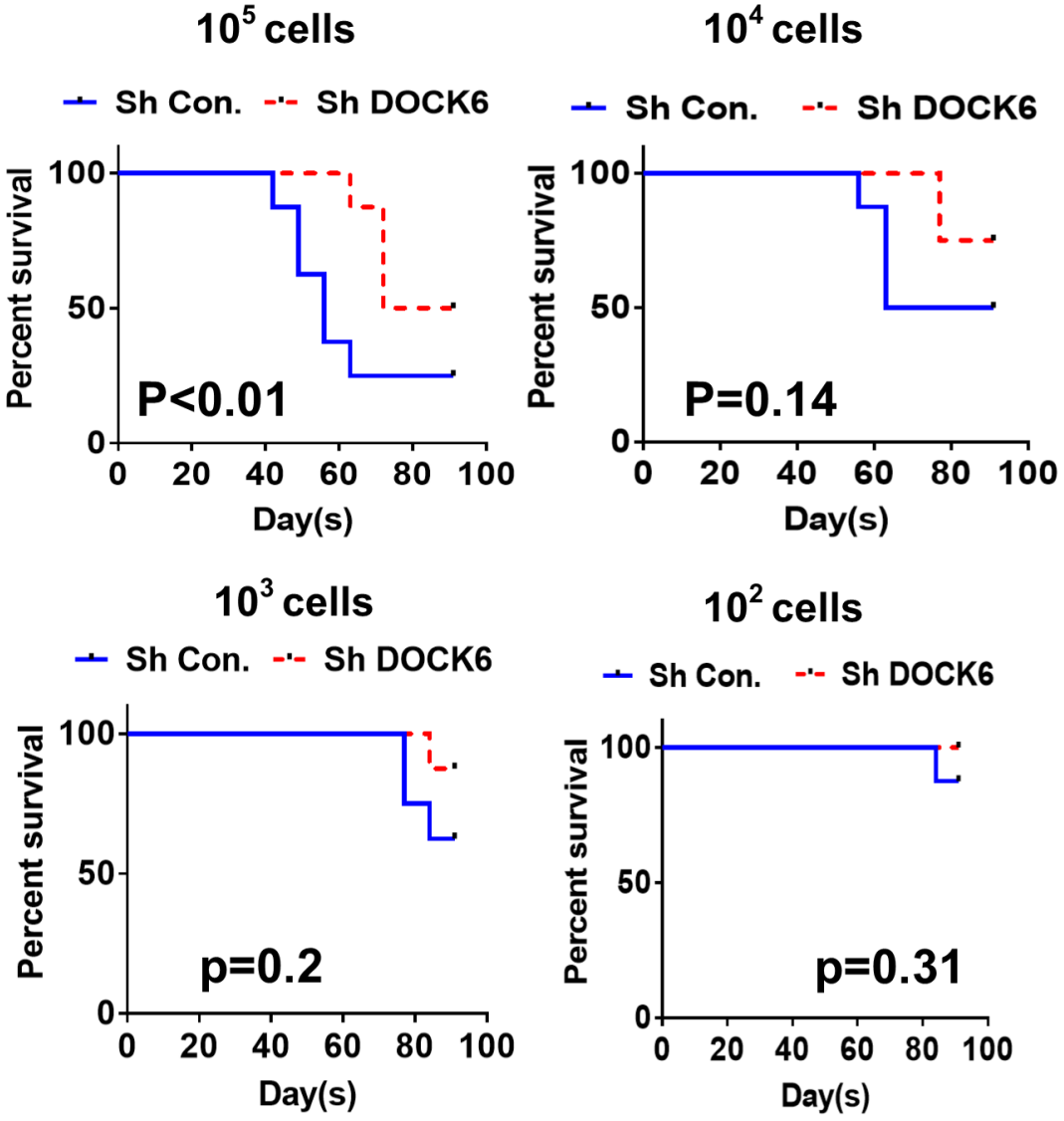

Supplemental Figure 6. DOCK6 silencing displays significantly weaker tumorigenic capacity

The cumulated tumor-free survival curves of nude mice injected with the indicated number of DOCK6-depleted and control AGS cells. Kaplan-Meier plots using standard tumor sizes (600mm^3) as a criterium for euthanasia.

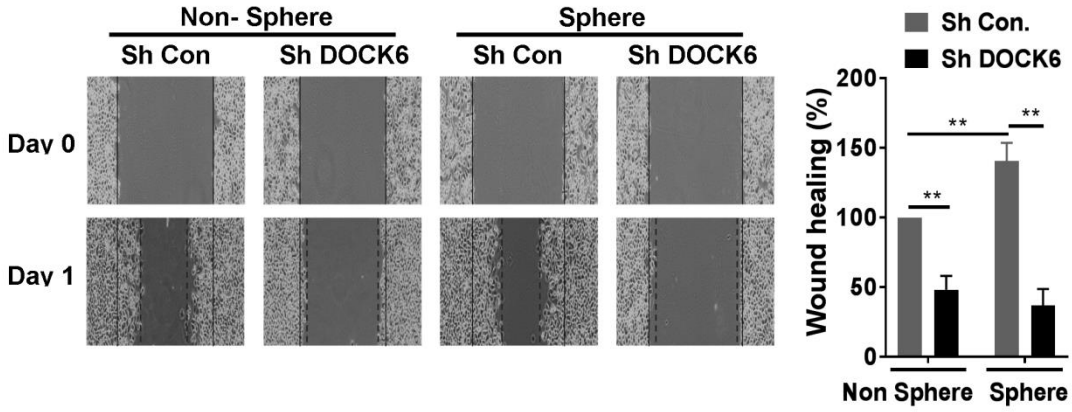

Supplemental Figure 7. DOCK6 silencing suppresses cell migration of GC-CSC cells

Wound healing assays of non-sphere and oncosphere-forming AGS cells with or without DOCK6 silencing. Right panel: quantified results.

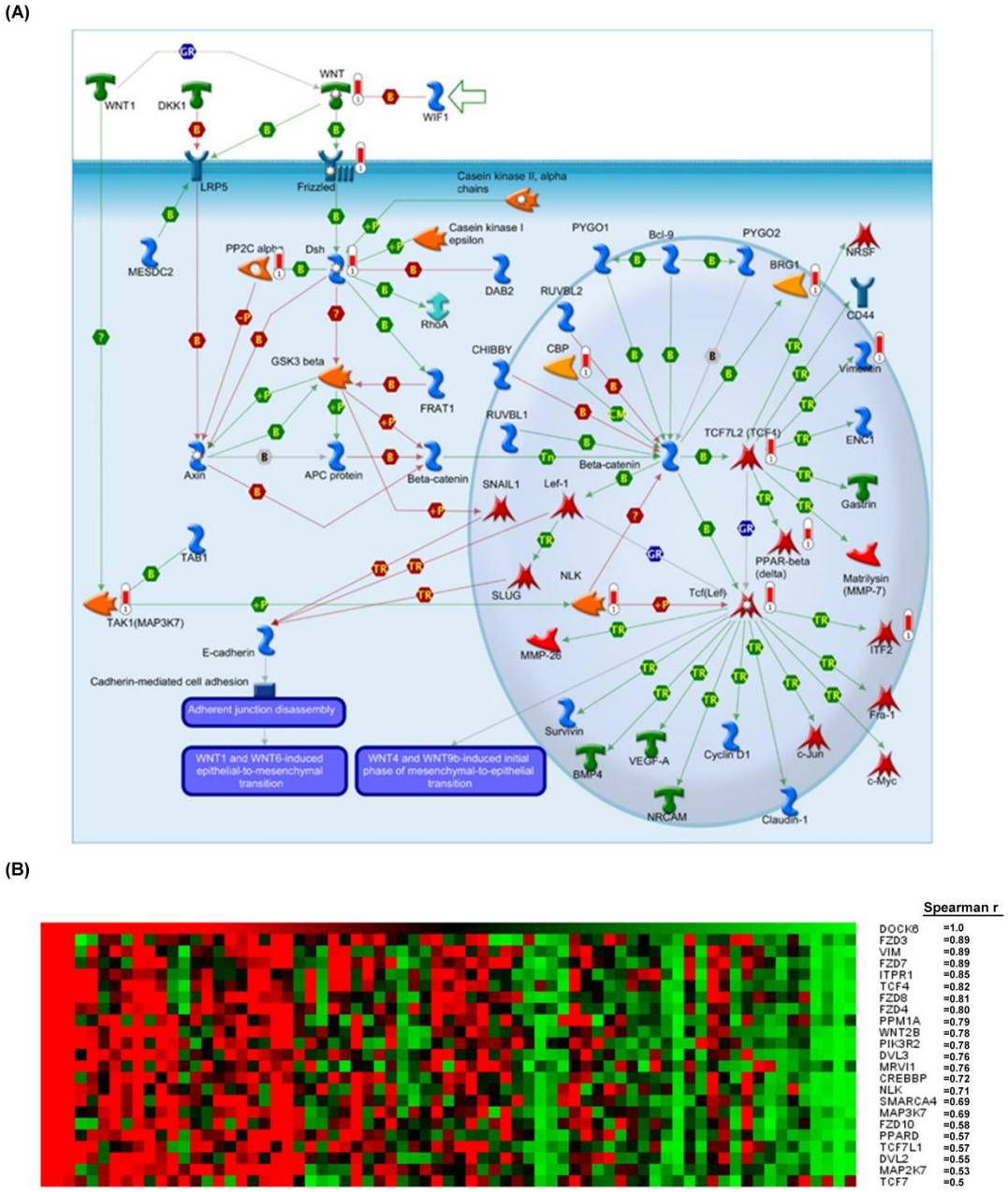

Supplemental Figure 8. DOCK6 is correlated with WNT/β-catenin signaling pathway by MetaCore analysis.

(A) MetaCore analysis of DOCK6 co-expressed genes from 3 gastric cancer datasets in WNT signaling pathway. (B) A heat map of expression profiles for WNT related genes of 71 human gastric adenocarcinomas from Cho dataset (GSE13861). Spearman rank correlation coefficient of individual genes with *DOCK6* shown in the right.

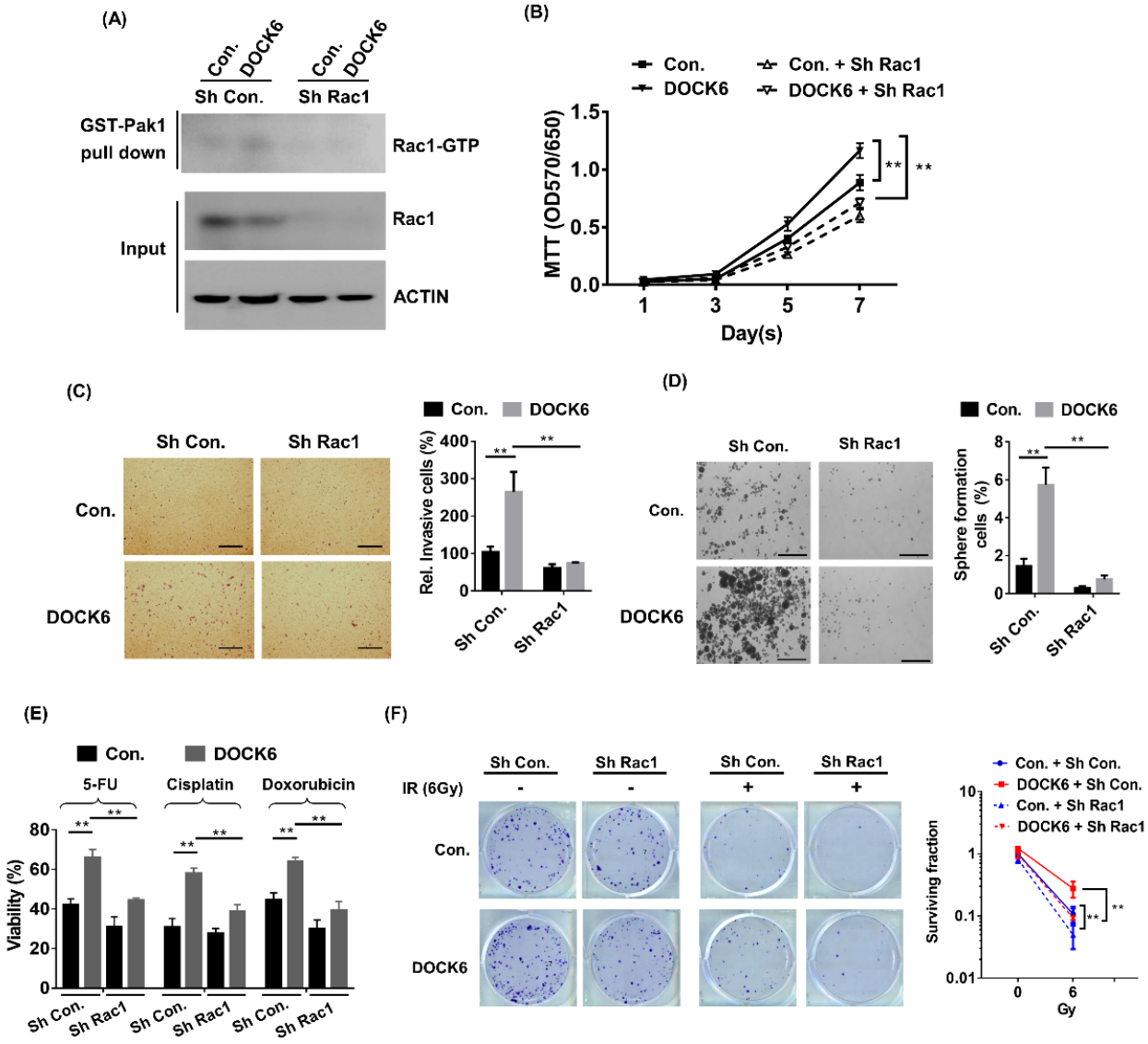

Supplemental Figure 9. Silence of Rac1 suppresses DOCK6 triggered GC proliferation, Matrigel invasion and chemo- and radio-resistance

(A) Immunoblotting analyses of Rac1-GTP and total Rac1 in DOCK6-overexpressing and control TMK-1 cells. (B) Measurement of cell growth curves with the MTT assay. (C) Transwell invasion assays of DOCK6-overexpressing and control TMK-1 cells with/without knockdown of Rac1. Right panel: quantified results. (Scale bar, 200 μm) (D) The oncosphere formation capacities of DOCK6-overexpressing and control TMK-1 cells with/without knockdown of Rac1. (Scale bar, 500 μm). The right panel represents statistical results. (E) Chemosensitivities of DOCK6-overexpressing and control TMK-1 cells with/without knockdown of Rac1 were determined based on the relative number of surviving cells after treatment with 5'FU (20 μg/ml), cisplatin (3 μM) or doxorubicin (1 μM) for 72 h. Cell survival was examined using the MTT method. (F) Representative photographs showing the growth characteristics of cell colonies 10 days after X-ray irradiation. The right panel represents the calculated clonogenic cell survival fraction.

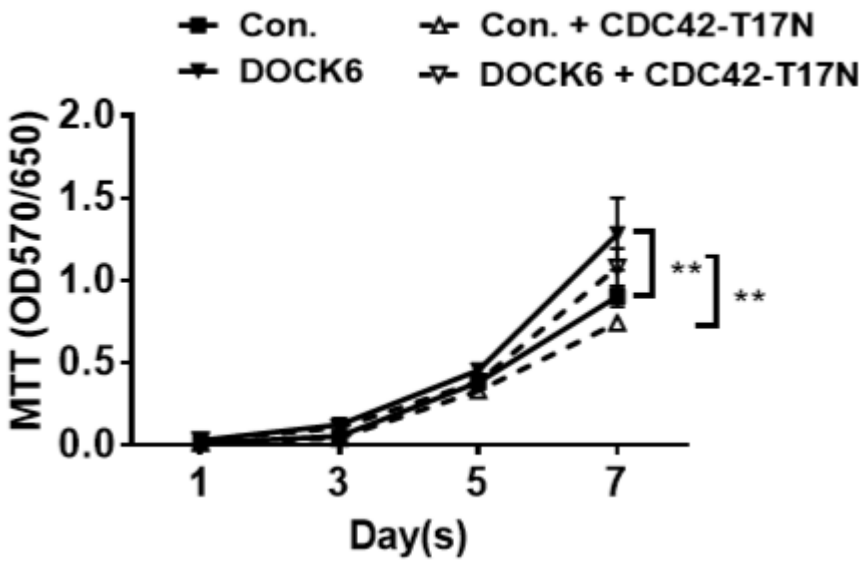

Supplemental Figure 10. CDC42-T17N overexpression exhibited the minor effects on DOCK6 triggered cell proliferation

Measurement of cell growth curves of DOCK6-overexpressing and control TMK-1 cells with/without CDC42-T17N overexpression with the MTT assay.